JACS
JOURNAL OF THE AMERICAN CHEMICAL SOCIETY

ARTICLE

pubs.acs.org/JACS

Mechanistic Insight into the Nitrosylation of the [4Fe−4S] Cluster of WhiB-like Proteins

Jason C. Crack,[†] Laura J. Smith,[§] Melanie R. Stapleton,[§] Jamie Peck,[†] Nicholas J. Watmough,[‡] Mark J. Buttner,[∥] Roger S. Buxton,[#] Jeffrey Green,[§] Vasily S. Oganesyan,[†] Andrew J. Thomson,[†] and Nick E. Le Brun*[,†]

Centre for Molecular and Structural Biochemistry, [†]School of Chemistry, and [‡]School of Biological Sciences, University of East Anglia, Norwich NR4 7TJ, United Kingdom

[§]The Krebs Institute, Department of Molecular Biology and Biotechnology, University of Sheffield, Sheffield S10 2TN, United Kingdom

[∥]Department of Molecular Microbiology, John Innes Centre, Norwich NR4 7UH, United Kingdom

[#]Division of Mycobacterial Research, MRC National Institute for Medical Research, Mill Hill, London NW7 1AA, United Kingdom

Supporting Information

ABSTRACT: The reactivity of protein bound iron−sulfur clusters with nitric oxide (NO) is well documented, but little is known about the actual mechanism of cluster nitrosylation. Here, we report studies of members of the Wbl family of [4Fe−4S] containing proteins, which play key roles in regulating developmental processes in actinomycetes, including *Streptomyces* and *Mycobacteria*, and have been shown to be NO responsive. *Streptomyces coelicolor* WhiD and *Mycobacterium tuberculosis* WhiB1 react extremely rapidly with NO in a multiphasic reaction involving, remarkably, 8 NO molecules per [4Fe−4S] cluster. The reaction is 10^4-fold faster than that observed with O_2 and is by far the most rapid iron−sulfur cluster nitrosylation reaction reported to date. An overall stoichiometry of $[Fe_4S_4(Cys)_4]^{2-} + 8NO \rightarrow 2[Fe^{I}_2(NO)_4(Cys)_2]^0 + S^{2-} + 3S^0$ has been established by determination of the sulfur products and their oxidation states. Kinetic analysis leads to a four-step mechanism that accounts for the observed NO dependence. DFT calculations suggest the possibility that the nitrosylation product is a novel cluster $[Fe^{I}_4(NO)_8(Cys)_4]^0$ derived by dimerization of a pair of Roussin's red ester (RRE) complexes.

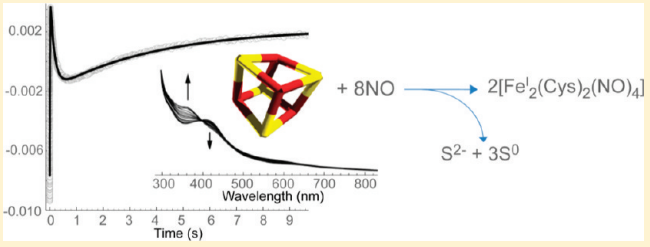

INTRODUCTION

Nitric oxide (NO) is a highly reactive, cytotoxic, lipophilic radical that readily reacts with a variety of redox proteins.[1,2] In eukaryotes, NO can function both in signaling (e.g., in vasodilation) and as a defense molecule within mammalian macrophages, fully exploiting its cytotoxic effects to combat pathogenic bacteria.[3] Many soil bacteria are exposed to NO, via the action of denitrifying species, such as *P. denitrificans*.[4] To survive the deleterious effects of NO, most bacteria, both pathogenic and benign, have evolved a suite of specific proteins to sense and detoxify NO.[5] Chemically, the cytotoxic effects of NO may involve processes such as S-nitrosylation of thiols,[6,7] N-nitrosylation of certain amino acids (e.g., tryptophan),[8] or nitrosative DNA damage.[9] In its signaling role, the direct interaction of NO with metal-containing cofactors is exploited.[2] For example, the reversible binding of NO to a heme group underlies its role in activating guanylate cyclase to generate cGMP and facilitate vasodilatation.[10] The bacterial transcriptional regulators NsrR, SoxR, and FNR, which all contain an iron−sulfur cluster, are involved in coordinating a physiological response to NO.[11−15]

Iron−sulfur proteins participate in many important cellular functions, but are also highly susceptible to NO-mediated damage.[16] Typically, this results in a tetrahedral $[Fe^{I}(NO)_2(SR)_2]^-$ species, in which RS^- are cysteinate ligands provided by the protein.[16,17] This species, termed a dinitrosyl iron complex (DNIC), possesses an unpaired electron, which gives rise to a distinctive EPR signal at $g = 2.03$[17] that has been used to follow DNIC formation from iron−sulfur clusters both in vivo[18] and in vitro.[15,19] Invariably, integration of such EPR signals has revealed spin intensity values substantially less than one unpaired electron per iron, implying a degradative process involving partial loss of both iron and sulfide ions from the cluster. A long list of examples has documented the substoichiometric nature of this reaction, irrespective of the type of iron−sulfur cluster, [2Fe−2S], [3Fe−4S], or [4Fe−4S], and cluster ligation; these include mammalian ferrochelatase,[20] various dehydratases,[19,21] HiPIP,[22] endonuclease III,[21] and NsrR.[13] However, inorganic studies have shown that an EPR silent, dinuclear iron tetra-nitrosyl species,

Received: October 25, 2010
Published: December 23, 2010

dx.doi.org/10.1021/ja109581t | J. Am. Chem. Soc. 2011, 133, 1112–1121

$[Fe^{I}_2(NO)_4(SR)_2]$, known as Roussin's red ester (RRE), can also be obtained following the reaction of NO with model iron−sulfur clusters.[23] The presence of this species in iron−sulfur proteins following exposure to NO has largely gone undocumented.

Streptomycetes are a group of nonmotile, spore forming, soil dwelling bacteria that are the most abundant source of clinically important antibiotics and other bioactive molecules to date. They contain a homologue of NsrR involved in coordinating NO detoxification.[13] Recent analysis of the *S. coelicolor* genome suggests that NsrR may also influence antibiotic production and the timing of sporulation in response to NO.[24] Interestingly, WhiD, a member of the WhiB-like (Wbl) family of [4Fe-4S] proteins that are found exclusively in actinomycetes, is required for the later stages of sporulation.[25−27] Other Wbl proteins appear to be involved in regulation of antibiotic production (WblA), antibiotic resistance (WblC), as well as septation (WhiB) during sporulation.[25,28,29] In *M. tuberculosis*, Wbl proteins have been implicated in the ability of this pathogen to persist within its host for long periods of time despite the low nutrient and oxidative nature of the granulome, as well as its remarkable tolerance of a wide range of antibiotics.[29−31] Various studies have demonstrated that, in response to hypoxia and NO exposure, *M. tuberculosis* accumulates triacylgerol, which is also present in the sputum of tuberculosis patients.[32,33] Recently, WhiB3, the *M. tuberculosis* homologue of WhiD, has been shown to regulate lipid and polyketide biosynthesis, including triacylgerol accumulation, in vivo, in response to activated macrophages.[34,35] Recently, *M. tuberculosis* WhiB1 was shown to be essential and to bind specific DNA sequences following nitrosylation.[36] Thus, it is now clear that the reaction of NO with Wbl proteins is a significant signaling process.

Here, we report a kinetic and thermodynamic investigation of the reaction of NO with the [4Fe−4S] cluster of two Wbl proteins, revealing several unprecedented features in terms of the rate, mechanism, and products of the reaction, with possible wider implications for understanding the reaction of NO with iron sulfur cluster-containing proteins.

EXPERIMENTAL SECTION

Purification of Wbl Proteins. Soluble holo-WhiD was overproduced from plasmid pIJ6631 as a $(His)_6$-tagged protein in aerobic *E. coli* cultures (BL21 λDE3 Star, Novagen; 37 °C) and purified as previously described.[27] Apo-WhiD was generated as previously described.[27,37] *M. tuberculosis* WhiB1 was purified as previously described.[36]

Nitric Oxide Solutions. Stock solutions of the NO donor PROLI-NONOate (Cayman Chemicals) were prepared in 25 mM NaOH, quantified optically ($\varepsilon_{252\ nm}$ 8400 M^{-1} cm^{-1}), and calibrated as previously described.[15] Two different methods were used to introduce NO to samples. In the first, the sample was directly titrated with varying amounts of PROLI-NONOate ($t_{1/2}$ = 1.5 s) and incubated at an ambient temperature for 5 min prior to spectroscopic measurements. In the second, used principally for kinetic experiments, an aliquot of PROLI-NONOate was combined with assay buffer (20 mM Tris, 20 mM Mes, 20 mM Bis Tris propane, 100 mM NaCl, 5% (v/v) glycerol, pH 8.0) and allowed to decompose in a gastight syringe (Hamilton) to achieve the desired NO concentration.

Sulfur Determination. Elemental sulfur (S^0) was determined by Sörbo's method[38,39] (with the omission of Cu^{2+} ions) using the addition of cyanide ion to generate SCN^- that yields an absorption band at 460 nm on addition of Fe^{3+} ions. Samples (100 μL) were combined with an equal volume of 1 M aqueous NH_4OH (Fluka), 30 μL of 0.1 M of aqueous cyanide and incubated for 40 min at ambient temperature. Samples were then diluted to 1 mL with H_2O, and 125 μL of Sörbo's reagent [125 mM $Fe^{III}(NO_3)_3$ dissolved in 14% (v/v) HNO_3] was added. The mixture was incubated at ambient temperature for 2 min prior to measuring $A_{460\ nm}$.[39] Fe^{III}−thiocyanate concentrations were determined by reference to a calibration curve generated from a solution of sodium thiocyanate (99.9%, Sigma Aldrich) in the range of 0−200 μM and were treated as described above. Specificity for S^0 was confirmed by performing the assay in the presence of S^{2-}, glutathione, or S^0 generated in situ via the oxidation of S^{2-} by excess glutathiol (oxidized glutathione). For determinations of S^0 following NO additions, nitrosylated WhiD was freshly prepared by titration with PROLI-NONOate until the $\Delta A_{362\ nm}$ leveled off and was used immediately. Where necessary, low molecular weight reactants were removed from the sample via ultrafiltration using a 3 kDa molecular weight cut off (Viva spin, GE Healthcare) or gel filtration (PD10, GE Healthcare).

Other Quantitative Methods. WhiD concentrations were determined using the method of Bradford (BioRad),[40] with bovine serum albumin as the standard. The iron content was determined with Ferene, as previously described.[41] Sulfide ions (S^{2-}) were assayed prior to and after reaction with NO in two ways. The first was the method of Beinert for acid labile sulfide,[42] and the second utilized Ellman's reagent (DTNB), as described previously.[41] In the latter case, the TNB^{2-} anion, which has a yellow color, displayed a slightly shifted absorbance maximum (λ_{max} = 420 nm) in the assay buffer, with $\varepsilon_{420\ nm}$ 13 200 M^{-1} cm^{-1}. In the presence of NO, TNB^{2-} slowly oxidizes back to DTNB even under anaerobic conditions.[43] Hence, a correction factor of 1.07 was applied to the TNB^{2-} concentration to account for this slow loss of ∼7% of TNB anions during the course of the assay.

Spectroscopy. UV−visible absorbance measurements were made with a Jasco V500 spectrometer, and CD spectra were measured with a Jasco J810 spectropolarimeter. X-band EPR spectra were recorded with a Bruker EMX spectrometer equipped with a TE-102 microwave cavity and an ESR-900 helium flow cryostat (Oxford Instruments). Spin intensities of paramagnetic samples were estimated by double integration of EPR spectra using 1 mM Cu(II), 10 mM EDTA as the standard. Fluorescence measurements were made using an anaerobic fluorescence cell (1 cm path length) in a Perkin-Elmer LS55 spectrometer.

Rapid Reaction Kinetics. UV−vis stopped-flow experiments were performed with an Applied Photophysics Bio-Sequential DX.17 MV spectrophotometer with a 1 cm path length cell. Absorption changes were detected either with a photomultiplier at a single wavelength or using a photodiode array from 340 to 460 nm. Fluorescence stopped-flow was performed with an excitation wavelength of 280 nm and a 305 nm cut off emission filter. The measured fluorescence intensity was the sum of the tryptophan emission envelope ($\sum I_{Trp}$), improving signal-to-noise. All stopped-flow experiments were carried out in assay buffer (20 mM Tris, 20 mM Mes, 20 mM Bis Tris Propane, 100 mM NaCl, 5% (v/v) glycerol, pH 8.0) using gastight syringes (Hamilton). Prior to use, the stopped-flow system was flushed with ∼30 mL of anaerobic buffer. All solutions used for stopped-flow experiments were stored and manipulated inside an anaerobic cabinet (Belle Technology). NO solutions were prepared as described above. The kinetic data were analyzed with the programs Origin (Microcal) and Dynafit.[44]

DFT Calculations. Spin-restricted DFT calculations were performed using the Gaussian 03 (Gaussian Inc.) computational package in conjunction with Becke's three parameter exchange functional (B3)[45] and the correlation functional of Lee, Yang, and Parr (LYP).[46] For iron and sulfur, the Hay and Wadt LANL2DZ basis set[47,48] with effective core potential (ECP) was employed. In the case of iron, the two outer p functions were replaced with reoptimized 4p functions in accordance with the previously reported procedure.[49] For sulfur, additional p and d polarization functions were added.[50] For carbon, oxygen, and nitrogen, an all electron 6-31+G(d,p) basis set was used, while for hydrogen

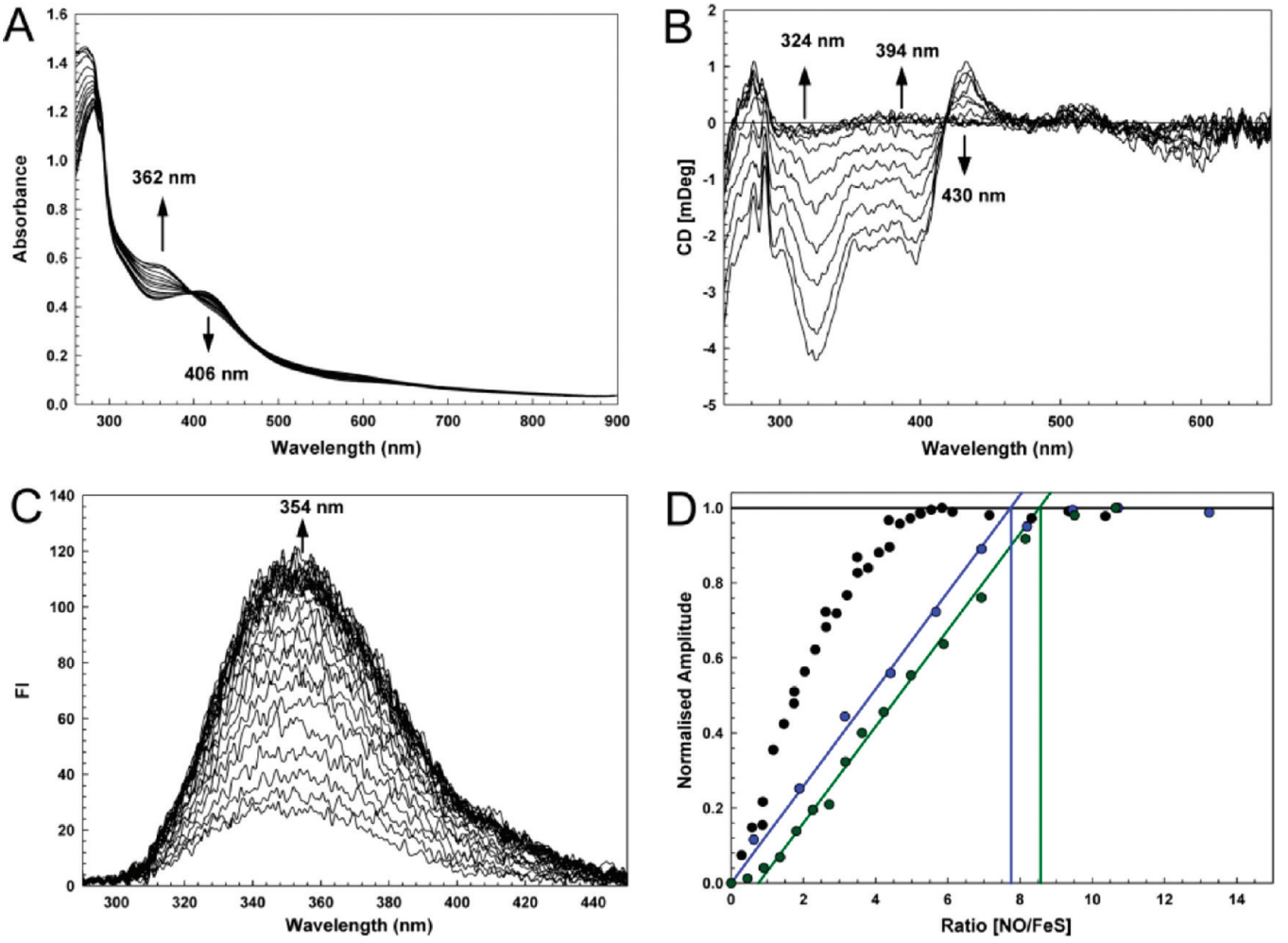

Figure 1. Titration of [4Fe−4S] WhiD with NO. (A) Absorbance spectra of [4Fe−4S] WhiD (29 μM) following additions of NO giving [NO]/[WhiD] ratios up to 11.5. (B) CD spectra of a titration equivalent to that in (A). (C) Fluorescence spectra of WhiD (1.9 μM; excitation at 280 nm; excitation and emission slit widths of 3 and 4 nm, respectively) following additions of NO giving [NO]/[WhiD] ratios up to 10.4. (D) Changes in the optical spectra, $\Delta A_{362\ nm}$ (green ●), $\Delta CD_{324\ nm}$ (blue ●), and $\Delta FI_{354\ nm}$ (●), were normalized and plotted versus the [NO]:[4Fe−4S] cluster ratio. Tangents to the initial slope and the titration end points of the absorbance and CD data are drawn in. The buffer was 20 mM Tris, 20 mM Bis-Tris-propane, 20 mM MES, 100 mM NaCl, and 5% glycerol pH 8.0.

atoms a 6-31G(d) basis set was employed. Structures were geometry optimized in the gas phase with the following symmetries imposed: the cis and trans conformers of the RRE $[Fe^{I}_2(NO)_4(Cys)_2]$ were constrained to C_{2v} and C_{2h} respectively, while the postulated octa-nitrosyl cluster $[Fe^{I}_4(NO)_8(Cys)_4]$ was constrained to D_{2d}.

RESULTS

The [4Fe−4S] Cluster of WhiD Reacts with Eight NO Molecules. Sequential additions of the NO releasing reagent PROLI-NONOate to an anaerobic sample of holo-WhiD were followed by UV−visible absorption and by near UV−visible CD spectroscopy; see Figure 1A and B. The progressive decrease in absorbance at 406 nm, the increase in the absorbance at 362 nm, and the lesser increase in the region 500−700 nm gave apparent isosbestic points at 398, 480, and 700 nm. A plot of $\Delta A_{362\ nm}$ against the ratio [NO]:[4Fe−4S] (Figure 1D) revealed that the reaction went to completion with a stoichiometry of 8.6 (±0.25) NO molecules per [4Fe−4S] cluster. CD signals arising from the cluster decreased almost to zero as the reaction with NO proceeded. A plot of the CD intensity at 324 nm against the ratio [NO]:[4Fe−4S] gave a similar reaction stoichiometry of 7.8 (±0.5) NO molecules per [4Fe−4S] cluster (Figure 1D). The final UV−visible spectrum (Figure 1A) was similar to that of an RRE,[15,17] with a principal absorption band at 362 nm and a shoulder at ∼430 nm. Based on a model compound extinction coefficient ($\varepsilon_{362\ nm}$ = 8530 M^{-1} cm^{-1},[17] the spectrum indicated the presence of two RREs per WhiD, consistent with the observed reaction stoichiometry. The WhiD NO reaction product was stable for many hours under anaerobic conditions, but was slowly lost in aerobic buffers.

The reaction was also monitored via protein tryptophan fluorescence ($FI_{354\ nm}$). Although WhiD contains three tryptophan residues, the fluorescence is almost completely quenched by the $[4Fe−4S]^{2+}$ cluster; see Figure 1C. As NO was added, the fluorescence intensity increased, reaching a maximum value that was ∼17% of the intensity recorded for apo-WhiD under identical conditions, indicating that the reaction product remains an efficient quencher of fluorescence intensity. A plot of $\Delta FI_{354\ nm}$ against the ratio [NO]:[4Fe−4S] showed no further changes at [NO]:[4Fe−4S] ≥ 4 (see Figure 1D), well before the

dx.doi.org/10.1021/ja109581t |J. Am. Chem. Soc. 2011, 133, 1112–1121

overall reaction was complete, indicating that the reaction is complex, and suggesting intermediate species may be detectable.

An EPR titration of [4Fe−4S] WhiD with NO was conducted under conditions identical to those of the UV−visible absorption titration above. Spectra, at 77 K, of WhiD at increasing levels of NO gave a signal at $g \approx 2.03$ (Figure S1). Quantification of the signal recorded with excess NO gave a concentration corresponding to only ∼10% of the original cluster (or <3% of the original iron). The far UV CD spectrum of [4Fe−4S] WhiD was consistent with a mainly α-helical protein, as previously reported (see Figure S2).[27] Addition of an excess of NO resulted in significant changes consistent with the partial loss of secondary structure (Figure S2).

The [4Fe−4S] Cluster of Wbl Proteins Reacts Extremely Rapidly with NO. The kinetics of the reaction of [4Fe−4S] WhiD with NO in excess were measured using stopped-flow by monitoring $A_{360\ nm}$ and $A_{420\ nm}$ at, or close to, the maxima of nitrosylated product and the iron−sulfur cluster reactant, respectively, and by measurement of tryptophan fluorescence (Figure 2). Three distinct kinetic phases were observed at both wavelengths in absorbance, and by fluorescence, suggesting a three-step reaction, A → B → C → D. The data were fitted separately, and together, to exponential functions (Figure 2A, B, and D), giving equivalent results. Each absorbance data set gave similar apparent rate constants for the initial, rapid phase and the final, slower phase of the NO reaction. Plots of the observed pseudofirst-order rate constants (k_{obs}) against NO concentration were linear for each step, indicating a first-order dependence on NO (see Figure 3A−D). However, the intermediate phase had quite different kinetic characteristics at 360 nm as compared to 420 nm, indicating that these two wavelengths report different processes in the intermediate part of the reaction. Therefore, the overall reaction should be modeled as a four-step reaction, that is, A → B → C → D → E, where the initial and final steps A → B and D → E, respectively, are detected at both wavelengths, while step B → C is detected at 360 nm and step C → D at 420 nm. The fluorescence response indicated that species B and C have similar quenching properties, resulting in a lag in the fluorescence recovery, and that D and E have similar fluorescence properties such that the final step, D → E, was not detected by fluorescence, consistent with the fluorescence titration data (Figure 1). The kinetic data are summarized in Table 1.

The amino acid sequence of *M. tuberculosis* WhiB1 is 43% identical to WhiD, also binds a [4Fe−4S] cluster, and becomes activated for specific DNA binding through reaction with ∼8 NO molecules per cluster.[36] Stopped-flow experiments revealed behavior similar to that of WhiD; see Figure 4 and Table 1. Therefore, we conclude that the reaction of NO with the [4Fe−4S] clusters of these two Wbl family proteins proceeds via the same mechanism.

Sulfur (S^0) Is Generated during the [4Fe−4S] WhiD Nitrosylation Reaction. Addition of NO to iron to generate DNIC/RRE species results in reduction of iron, most commonly to the Fe(I) state. When an iron−sulfur cluster is present, the electron(s) required may come from the oxidation of cluster sulfide ion, S^{2-}, to S^0. Apo-WhiD was found to contain almost no S^{2-} (Table 2), but slightly higher amounts of S^0, 0.25 (±0.02) per protein. Analysis of holo-WhiD before reaction with NO gave the expected ratio of S^{2-} to [4Fe−4S] cluster of 4.00 (±0.04). S^0 content of the holo-protein could not be reliably determined due to cluster instability under assay conditions. After reaction with excess NO, the product was found to contain 0.31 (±0.02) S^{2-} and 3.24 (±0.18) S^0 per [4Fe−4S] (Table 3), demonstrating that S^0 is generated during the nitrosylation reaction by S^{2-} oxidation.

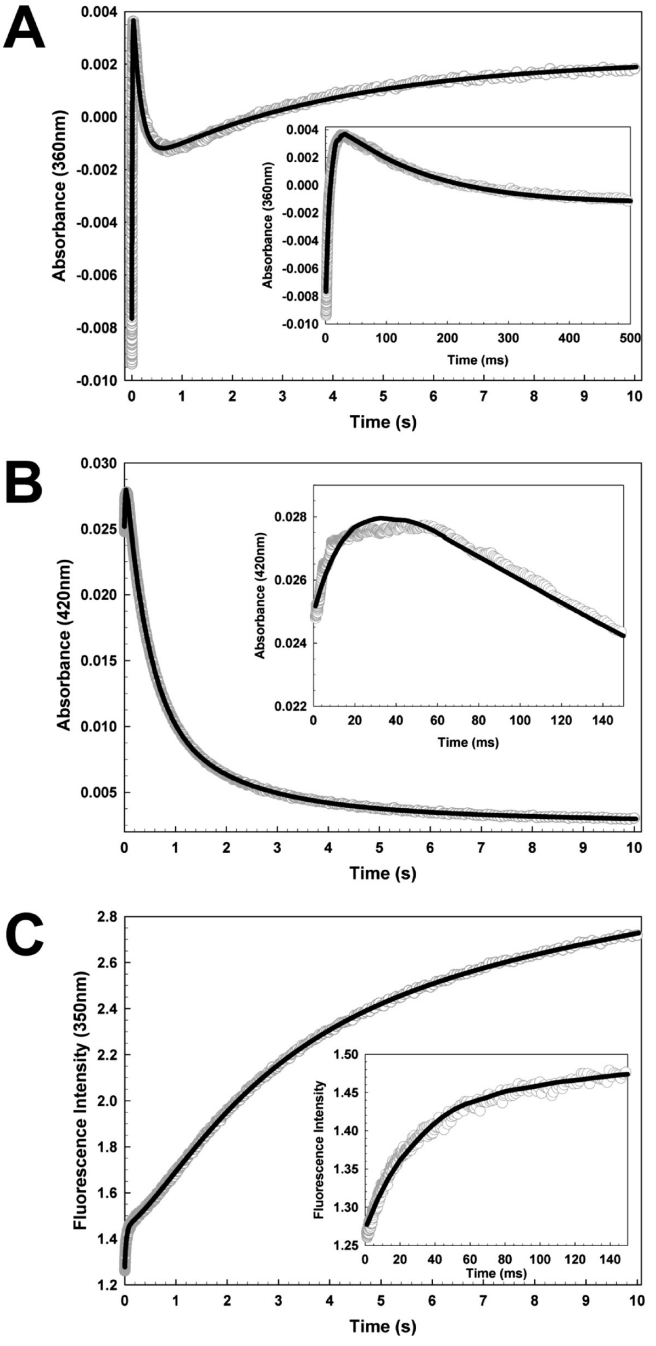

Figure 2. Stopped-flow kinetics of [4Fe−4S] WhiD nitrosylation. Stopped-flow kinetic traces following absorbance at (A) 360 nm and (B) 420 nm were recorded with WhiD (7.0 μM [4Fe−4S]) in the presence of 247 μM NO, giving a [NO]/[4Fe−4S] ratio of ∼35. (C) Stopped-flow kinetics traces following fluorescence changes upon mixing WhiD (2.0 μM [4Fe−4S]) with 145 μM NO, [NO]/[4Fe−4S] ratio of ∼72. Fits to each of the observed phases are drawn in (black lines). Insets show early events in the reaction time course.

The release of S^{2-} during iron−sulfur cluster conversion was also followed by reaction with DTNB.[27] DTNB did not affect the stability of the WhiD cluster, but gave rise to spectral changes due to the release of the TNB anion following reaction of DTNB with the apoprotein component (up to 30%) of the WhiD sample.

dx.doi.org/10.1021/ja109581t | J. Am. Chem. Soc. 2011, 133, 1112–1121

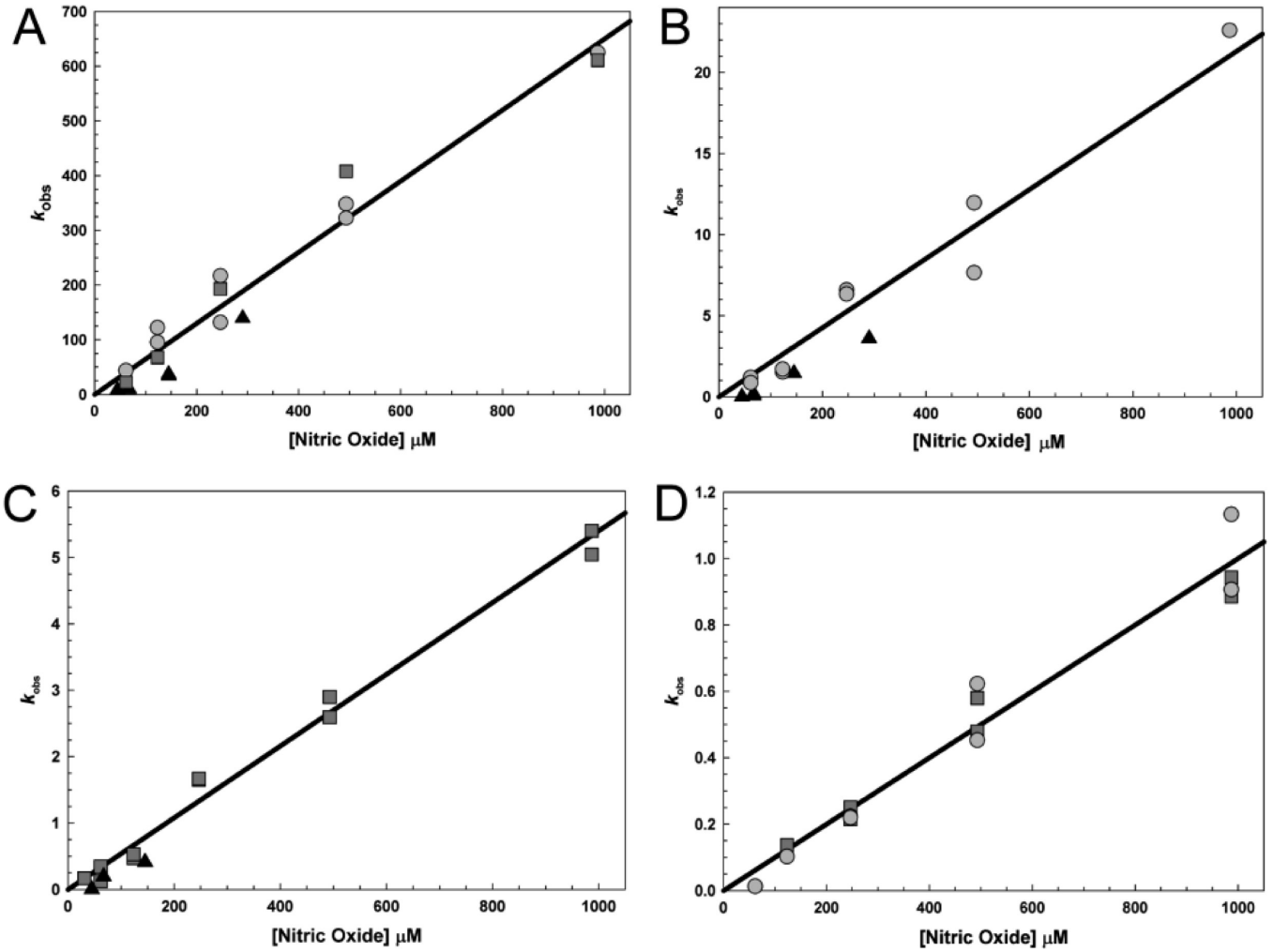

Figure 3. Kinetic dependencies of the nitrosylation reaction on NO concentration. (A−D) Plots of the observed (pseudofirst order) rate constants (k_{obs}) obtained from fits of the kinetic data in Figure 2 at 360 and 420 nm, over a range of NO concentrations. Panels A−D correspond to steps 1−4, respectively. k_{obs} corresponds to $A_{362\ nm}$ (light gray ●), $A_{420\ nm}$ (dark gray ■), and fluorescence (▲). Least-squares linear fits of the data are shown (black line), the gradient of which corresponds to the apparent second-order rate constant.

Table 1. Rate Constants for the Reaction of Wbl Proteins with NO

	rate constant ($M^{-1}\ s^{-1}$)[a]	
reaction step	WhiD	WhiB1
A → B	$(6.50 \pm 0.18) \times 10^5$	$(4.40 \pm 0.44) \times 10^5$
B → C	$(2.13 \pm 0.12) \times 10^4$	$(1.38 \pm 0.04) \times 10^4$
C → D	$(5.36 \pm 0.14) \times 10^3$	$(8.34 \pm 0.93) \times 10^3$
D → E	$(1.00 \pm 0.03) \times 10^3$	$(0.90 \pm 0.06) \times 10^3$

[a] Derived from linear fits of the data in Figure 3 (*S. coelicolor* WhiD) and Figure 4 (*M. tuberculosis* WhiB1), respectively.

As isolated, the apo-WhiD component contained 0.90 (±0.07) available thiols per protein (see Figure 5A and Table 4). Apo-Wbl proteins, including WhiD and WhiB1, have previously been shown to form both intra- and/or intermolecular disulfide bonds, thus decreasing from four the number of reactive cysteine thiol groups. The introduction of NO caused a further change in the spectrum of the WhiD/DTNB mixture due to the release of additional TNB anions (see Figure 5B). Because DTNB is inert to NO, the observed reaction is attributed to changes in WhiD following cluster nitrosylation. Overall, cluster nitrosylation led to the release of 1.20 (±0.12) S^{2-} per cluster (Table 4), indicating that approximately three out of four sulfide ions were unavailable for reaction with DTNB. This is consistent with the S^0 assays, which also indicated that approximately three S^0 are generated per cluster during the nitrosylation reaction (Table 3).

Nitrosylated Cluster Products Remain Associated with WhiD. An NO titration of WhiD in the presence of a 2-fold excess of EDTA gave results identical to those in Figure 1A, indicating that the nitrosylated product was stable (Figure S3). After ultrafiltration or gel filtration to remove weakly or unbound species following exposure of holo-WhiD to NO, the UV−visible spectrum of the protein was identical in form to that recorded prior to separation, but of lower intensity, indicating that approximately one-half of the nitrosylated species had been lost, and this was confirmed by iron analysis (~2.24 iron ions remaining per original [4Fe−4S] cluster). Interestingly, although S^{2-} was low (~0.25 per cluster), a significant amount of S^0 (~2−2.75 S^0 per cluster, depending on the method of separation) remained associated with WhiD, possibly as persulfide (Table 3).

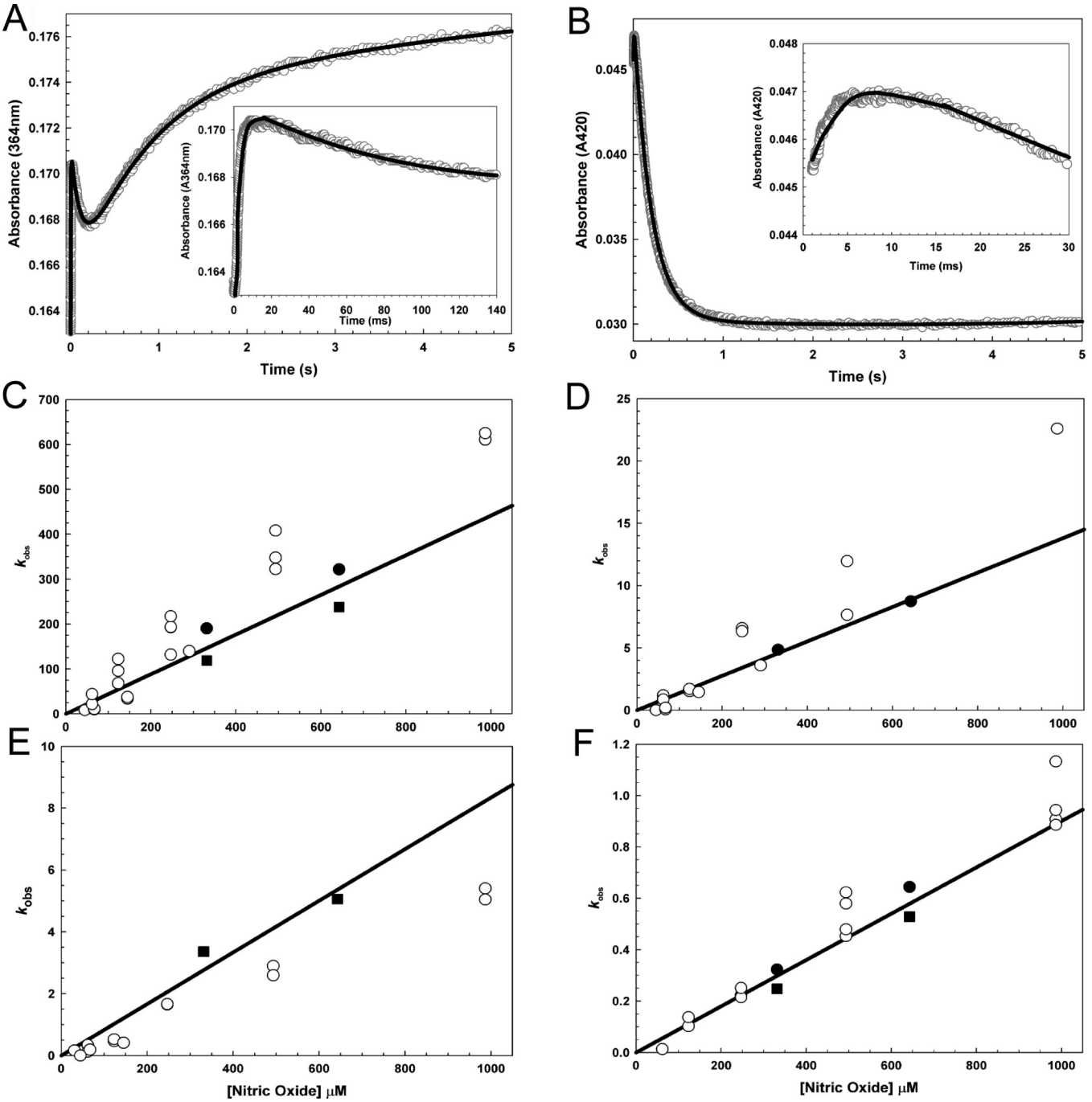

Figure 4. Stopped-flow kinetics of [4Fe−4S] *M. tuberculosis* WhiB1 nitrosylation. Stopped-flow kinetic traces following absorbance at (A) 364 nm and (B) 420 nm were recorded with WhiB1 (7.0 μM [4Fe−4S]) in the presence of 643 μM NO, giving a [NO]/[4Fe−4S] ratio of ∼92. Fits to each of the observed phases are drawn in (black lines). Insets show early events in the reaction time course. (C−F) Multiphase kinetics was observed for the reaction of [4Fe−4S] WhiB1 with NO over a range of concentrations (under pseudofirst-order conditions) at both 364 and 420 nm and observed rate constants (k_{obs}) plotted as a function of NO concentration. Panels C−F corresponds to steps 1−4, respectively, of the four-step mechanism described in the text. k_{obs} corresponds to $A_{364\ nm}$ (●) and $A_{420\ nm}$ (■). Least-squares linear fits of the data are shown (black line), the gradient of which corresponds to the apparent second-order rate constant. Data for *S. coelicolor* WhiD, from Figure 3, are plotted for comparison (○). Overall, the data for WhiB1 were very similar to those for WhiD (see Table 1).

We conclude that the product of nitrosylation is rather unstable to manipulation, readily undergoing conversion to a single RRE species.

■ DISCUSSION

Although the reactivity of NO toward protein bound iron−sulfur clusters has been studied for many years, the chemical identities of the products have not been well characterized, and few studies have been reported of the kinetics and mechanism of the reaction. Two examples illustrate this. The reaction of the four cysteine-coordinated HiPiP [4Fe−4S] cluster with NO was studied by Cowan et al.[22] using optical and EPR spectroscopy and mass spectrometry. They concluded that two DNICs were

dx.doi.org/10.1021/ja109581t |*J. Am. Chem. Soc.* 2011, 133, 1112–1121

Table 2. Sulfide (S^{2-}) and Sulfur (S^0) Content of Apo- and Holo-WhiD

sample	protein (μM)	S^{2-} (μM)	S^{2-}/sample	S^0 (μM)	S^0/sample
apo-WhiD[a]	248	9.6 (±0.01)	0.04 (±0.00)[b]	287 (±12)	1.16 (±0.49)[b]
apo-WhiD[c]	115	2.2 (±0.01)	0.02 (±0.00)[b]	28.4 (±2.6)	0.25 (±0.02)[b]
holo-WhiD[d]	28.0[e]	112 (±1.2)	4.00 (±0.04)[f]	n.d.[g]	n.d.

[a] Prepared according to Alam et al.[37] [b] Expressed as S^{2-} or S^0 per protein. [c] Prepared according to Crack et al.[27] The significantly higher amounts of S^0 observed in apo-WhiD prepared as described by Alam et al.[37] may be the origin of the disulfide reductase activity associated with apo-WhiD,[27] and possibly other Wbl proteins.[58] [d] Assayed under anaerobic conditions (≤2 ppm O_2). [e] Expressed as [4Fe−4S] cluster concentration. The sample contained 36 μM protein, 28 μM cluster. [f] Expressed as S^{2-} per cluster [g] n.d. = not determined.

Table 3. Sulfide (S^{2-})[a] and Sulfur (S^0) Content of NO-Treated Holo-WhiD

		before treatment with NO			after treatment with NO (~303 μM)			
sample	protein (μM)	[4Fe−4S] (μM)	S^{2-} (μM)	S^{2-}/[4Fe−4S]	S^{2-} (μM)	S^{2-}/[4Fe−4S]	S^0 (μM)	S^0/[4Fe−4S]
1	35.1	27.5	109.9 (±1.15)	4.00 (±0.04)	10.4 (±0.74)	0.38 (±0.04)	96.7 (±3.3)	3.52 (±0.12)
2	35.1	27.5	109.9 (±1.15)	4.00 (±0.04)	8.6 (±0.43)	0.32 (±0.02)	88.9 (±5.1)	3.23 (±0.18)
3[b]	44.6	28.0	112.0 (±1.15)	4.00 (±0.04)	n.d.[c]	n.d.	76.6 (±4.1)	2.74 (±0.15)
4[d]	32.4	25.4	102.0 (±1.15)	4.02 (±0.04)	5.7 (±0.93)	0.22 (±0.04)	50.8 (±5.9)	2.00 (±0.23)

[a] Measurements were made by the method of Beinert.[42] [b] Low molecular weight reactants and products were removed via gel filtration (PD10, GE Healthcare). [c] n.d. = not determined. [d] Low molecular weight reactants and products were removed via ultrafiltration (Vivaspin 500, 3 kDa MWCO, GE Healthcare).

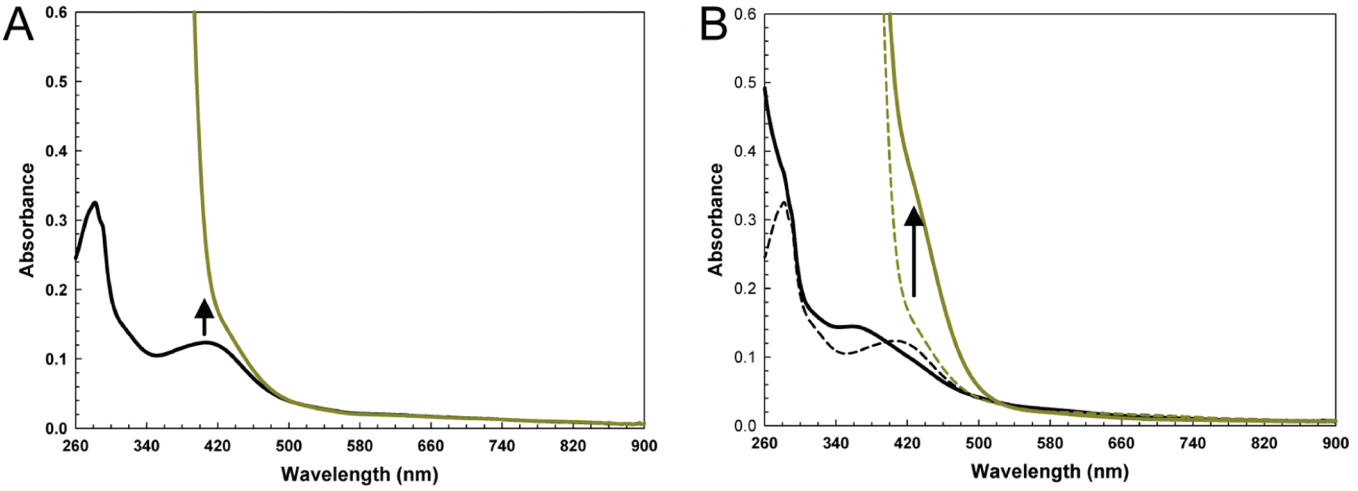

Figure 5. Quantification of sulfide release during WhiD cluster nitrosylation. (A) UV−visible absorbance spectra of 12.6 μM WhiD containing 7.9 μM [4Fe−4S] in assay buffer pH 8.0 before (solid black line) and after (solid olive green line) the addition of DTNB (192 μM final concentration). The arrow indicates $\Delta A_{420\ nm}$, which results from the free thiol content of the sample. (B) The sample in (A) (dashed black and olive lines) following the addition of NO, as PROLI-NONOate (final NO concentration 141.5 μM) (solid olive line). The spectrum in solid black resulted from an equivalent addition of NO, as PROLI-NONOate, to an identical sample in the absence of DTNB. From these two spectra, the $\Delta A_{420\ nm}$ due to sulfide released during cluster nitrosylation was calculated. A correction factor was applied to account for the slow loss (~7%) of TNB anions during the course of the assay.[43] In the assay buffer at pH 8.0, TNB anions displayed a slightly shifted absorbance maximum at 420 nm, with $\varepsilon_{420\ nm}$ = 13 200 M^{-1} cm^{-1}. All absorbance changes correspond to sample 3 in Table 4.

formed at a single cluster site, although the yield was well below (<60%) that expected from a stoichiometric reaction. More recently, Duan et al.[21] studied the reactivity of NO toward [4Fe−4S] clusters in dehydratases, bound by three cysteine ligands, and an endonuclease, with four cysteine ligands. They found that the reaction was slow in the latter and faster in the former and, in all cases, generated DNIC EPR signals with low spin intensities. Both studies, then, only identified (through characteristic EPR signals) DNIC species that were well below stoichiometric levels. The fate of the remainder of the cluster iron is unknown. Reaction of [4Fe−4S] FNR,[15] mitochondrial aconitase,[19] and [2Fe−2S] NsrR[13] with NO also resulted in low concentrations of DNICs, and evidence from UV−visible absorbance spectra, which contained a characteristic maximum at ~360 nm, strongly suggested the presence of significant quantities of an EPR silent RRE, $[Fe_2(NO)_4(Cys)_2]^0$. We note that RREs and DNIC species exist in an equilibrium that is highly dependent upon the concentration of the thiol ligand.[17]

Reaction of WhiD with NO, like *M. tuberculosis* WhiB1,[36] was complete at eight NO molecules per [4Fe−4S] cluster, yielding

Table 4. DTNB Determination of Sulfide Ion (S^{2-})[a] Released from NO-Treated Holo-WhiD

	anaerobic					after reaction with NO (~283 μM)				
sample	protein (μM)[b]	apo-protein (μM)	[4Fe−4S] (μM)	TNB (μM)[c]	thiol/ apo[d]	TNB (μM)	ΔTNB (μM)	S^{2-} (μM)[e]	S^{2-}/ [4Fe−4S]	S^{2-}/ [4Fe−4S][f,g]
1	12.6	4.7	7.9	4.53	0.96	23.62	19.10	9.55	1.21	1.29
2	12.5	4.7	7.8	4.66	0.98	19.33	14.77	7.39	0.95	1.01
3	12.6	4.7	7.9	4.01	0.86	22.56	18.55	9.28	1.18	1.26
4	11.8	4.4	7.4	3.80	0.86	21.42	17.61	8.81	1.19	1.27
5	11.3	4.2	7.1	3.50	0.83	19.06	15.56	7.78	1.10	1.17

[a] Determined using a DNTB assay.[41] [b] Used as isolated. Intra-/intermolecular disulfides were not reduced prior to assaying. [c] DTNB was added to the as isolated protein under nondenaturing anaerobic conditions. The concentration of TNB anions detected was assumed to correspond to the modification of all free thiol groups present in the sample. [d] Thiol groups react stoichiometrically with DTNB to generate TNB, and these are assumed to originate from apo-WhiD. [e] One sulfide ion reacts with DTNB to yield two TNB anions; see Nashef et al.[59] [f] NO can catalyze the formation of disulfide bonds, converting TNB to DTNB. This reaction is slow under anaerobic conditions.[43] Over the course of the assay, ~7% of the TNB anions formed were converted back to DTNB; hence a correction factor of 1.07 was applied to account for this loss. [g] Here, it was assumed that all of the cluster-coordinating cysteine residues were unavailable for reaction with DTNB because they remain coordinating iron (as in most DNIC species). However, if a proportion of cysteine thiol groups did become available, the DTNB assay would represent an overestimation of the S^{2-} released. This may account for the higher S^{2-} concentration obtained using DTNB as compared to the Beinert assay (Table 3).

a product with properties similar to an RRE.[15,17] Approximately one S^{2-} ion and three S^0 atoms were detected on completion of the nitrosylation reaction. Binding of the π-acid ligand NO to an iron−sulfur cluster will favor reduction of the iron. Six electrons are required to reduce the $[4Fe{-}4S]^{2+}$ core to four Fe(I) ions, and elemental analyses showed that S^{2-} is the sacrificial reductant, generating S^0 atoms. We note that a protein-associated form of Roussin's Black Salt (RBS), $[Fe_4S_3(NO)_7]^-$, was recently reported after NO treatment of the [4Fe−4S] cluster in the D143C form of the ferredoxin from *P. furiosus*.[51] Our S^0/S^{2-} analyses show that such a product cannot be formed here, as insufficient S^{2-} ions remain following nitrosylation. Thus, by making the assumption that all four cysteine thiolates that ligate the [4Fe−4S] cluster also bind the nitrosylated product(s) to the protein, a balanced equation can be written (eq 1).

$$[Fe^{II}{}_2Fe^{III}{}_2S_4(Cys)_4]^{2-} + 8NO \rightarrow 2[Fe^{I}{}_2(NO)_4(Cys)_2]^0 + S^{2-} + 3S^0 \quad (1)$$

The stopped-flow data revealed that WhiD/WhiB1 [4Fe−4S] nitrosylation proceeds via a complex, multiphasic reaction, with a rate at least ~4 orders of magnitude greater than for the reaction with O_2.[27,36] Mechanisms by which a protein environment can regulate the relative rates of attack of diatomic molecules on specific sites of an iron−sulfur clusters are poorly understood. Wbl proteins clearly offer an opportunity for further insight. The first step of the reaction of [4Fe−4S] WhiD/WhiB1 with NO (A → B; first order with respect to NO) is very likely the binding of one NO molecule to the cluster. This increases accessibility to further NO binding in steps B → C (detected at 360 nm) and C → D (detected at 420 nm). Both are also first order in NO, indicating either that a single NO is involved in each, or that NO binding to different irons of the cluster occurs independently, giving an overall first-order dependence. Step C → D may well be coupled to a cluster conformational rearrangement, because the major part of the fluorescence recovery occurs during this step. Both steps B → C and C → D resulted in a net decrease in absorbance, suggesting that iron−sulfide and/or iron−cysteine interactions (which give rise to the cluster absorbance) are significantly disrupted during these steps, but may also entail the reduction of iron (to the +1 state) and oxidation of S^{2-} (to S^0). We note that Harrop et al.[52] suggested that NO binding and S^{2-} oxidation occur concomitantly to yield S^0 during the formation of DNICs from model inorganic $[2Fe{-}2S]^{2+}$ clusters. Furthermore, the fluorescence titration data revealed a stable intermediate at a stoichiometry of ~4 NO molecules per [4Fe−4S] cluster. Thus, intermediate D appears to be a tetranitrosylated species. The last step of the reaction (D → E) was again first order in NO leading to an EPR-silent octa-nitrosylated product(s). The observed molecularity would be expected if each iron reacts independently with NO.

The formation of a pair of RREs raises the question of how they might fit within a protein cavity that previously accommodated a [4Fe−4S] cluster. Provided the protein binding site does not substantially reorder, the cluster binding cavity will contain an approximately tetrahedral array of ligating cysteines. A pair of RREs, having their Fe_2S_2 planes parallel but their Fe−Fe axes at 90° to one another, and with their thiols in the *cis* orientation relative to the Fe_2S_2 plane, would thus ligate a pseudotetrahedral array of thiols. Although crystallographic studies of RREs[53] showed the bridging thiolate ligands in the trans orientation, Glidewell and co-workers[54−56] reported variable-temperature NMR data that demonstrated the existence of cis and trans spatial isomers in solution. Geometry optimizations using density functional theory (DFT) performed on the cis and trans isomers of complex $[Fe^{I}{}_2(RS)_2(NO)_4]^0$ (R = *n*-Pr) gave an energy difference of only ~12 kJ mol^{-1}; see Figure 6A and B. Thus, a pair of cis RRE species forming a tetrahedral array of four Fe(I) ions within a pseudotetrahedral array of thiolates could fit within the protein cavity.

To examine how close a pair of RREs thus oriented could approach, and to estimate the stability of such an arrangement, we have carried out energy minimization calculations with respect to the S_4 axis through the pair using DFT. This resulted in a close approach that can be viewed as the novel cluster, $[Fe^{I}{}_4(NO)_8(SCH_3)_4]^0$ (Figure 6C). Although calculations of the free energy of formation indicate that such a species would be less stable (by ~280 kJ mol^{-1}) than a pair of essentially isolated RREs in vacuo, a protein template of tetrahedral thiols could exert a stabilizing effect. The analysis points to the possibility that complete

dx.doi.org/10.1021/ja109581t | *J. Am. Chem. Soc.* 2011, 133, 1112–1121

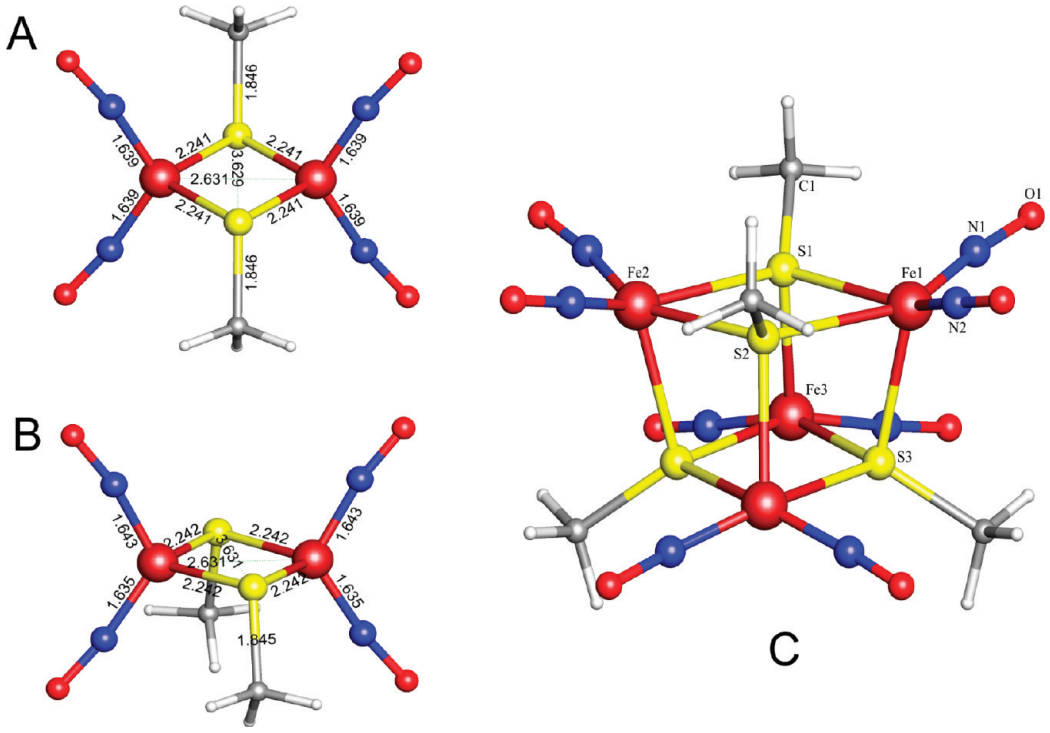

Figure 6. Roussin's red ester (RRE) and a proposed novel octa-nitrosyl cluster resulting from nitrosylation of the [4Fe−4S] cluster of Wbl proteins. DFT energy-minimized structures of RRE, $[Fe^{I}_{2}(NO)_{4}(CH_{3}S^{-})_{2}]^{0}$, with bridging methyl thiolates in the trans (A) and cis (B) conformations. Calculations revealed that, in vacuo, the cis and trans configurations have identical relative energies. Bond lengths (in Å) are indicated. (C) DFT energy-minimized structure of a pair RREs species, with bridging methyl thiolates, $[Fe^{I}_{4}(NO)_{8}(SCH_{3})_{4}]^{0}$, having an overall point symmetry of D_{2d} with the inter-RRE direction aligned along the S_4 axis. The $Fe(NO)_2$ unit lies in a plane that minimizes the steric interaction with the tricapping thiol groups. The Fe_4 unit is flattened from the regular T_d shape along the S_4 axis. This is apparent from the Fe−S distance of 2.37 Å that links the RREs as compared to a Fe−S distance of 2.54 Å within a RRE. Thus, the Fe−Fe distance across the rhomb increased from 2.63 to 3.02 Å, and the S−S distance increased from 3.63 to 4.07 Å; see Table S1 for full details of interatomic distances.

nitrosylation, with eight NO molecules, of a [4Fe−4S] cluster within a protein cavity could generate a novel cluster, $[Fe^{I}_{4}(NO)_{8}(S-cys)_{4}]^{0}$, resulting from the dimerization of a pair of RREs (see Figure S4 for a schematic view of the proposed nitrosylation mechanism). The experimental data showed that the nitrosylated product is converted to a single RRE following gel filtration or ultrafiltration. The formation of such an octa-nitrosylated species from a [4Fe−4S] cluster within a protein cavity would entail a rearrangement of the iron positions relative to the cysteine thiols, and hence could drive a protein conformational change to switch the DNA binding properties of a Wbl protein upon reaction with NO.[34−36] Far UV CD data (Figure S2) are consistent with a significant structural change upon reaction with NO.

Reaction of protein bound iron−sulfur clusters with NO, leading to iron nitrosylation and cluster disassembly, has long been recognized as a means by which this gas exerts its toxic effect. It is clearly also a means by which bacteria sense NO,[24] and although the precise role(s) of the Wbl protein family in actinomycetes has remained uncertain for sometime,[57] strong evidence is now accumulating that these are DNA-binding regulatory proteins, and that some, at least, are associated with responses to nitrosative stress.[34−36] Importantly, *M. tuberculosis* WhiB1 was recently shown to be a NO-responsive regulator that has very low affinity for DNA in its [4Fe−4S] cluster form, but bound DNA specifically in its nitrosylated form.[36] The present work provides the first detailed analysis of the mechanism by which NO attacks protein-bound iron−sulfur clusters, with unexpected outcomes in terms of the number of NO molecules involved and in the fast rate with which reaction goes to completion. The similarity of the reactions to NO of *S. coelicolor* WhiD and *M. tuberculosis* WhiB1 indicates both that the reaction has biological significance, with both proteins displaying a very significant preference for reaction with NO as compared to ROS, and that the mechanism of nitrosylation is conserved, at least within members of the Wbl family. In the case of WhiB1, nitrosylation altered the DNA-binding ability of the protein,[36] which, together with the present work, provides a clear framework for understanding the molecular details of regulation.

■ ASSOCIATED CONTENT

Supporting Information. [4Fe−4S] WhiD nitrosylation followed by EPR spectroscopy (Figure S1); far UV CD spectra of [4Fe−4S] WhiD before and after NO treatment (Figure S2); titration of [4Fe−4S] WhiD with NO in the presence of the iron-chelator EDTA (Figure S3); scheme illustrating the nitrosylation of a Wbl-protein bound [4Fe−4S] cluster (Figure S4); and distances and angles in *cis* and *trans* RREs and a novel octa-nitrosyl species (Table S1). This material is available free of charge via the Internet at http://pubs.acs.org.

■ AUTHOR INFORMATION

Corresponding Author
n.le-brun@uea.ac.uk

■ ACKNOWLEDGMENT

This work was supported by UK BBSRC grants BB/G019347/1 and BB/D00926X/1 and Wellcome Trust grant 078731/Z/05/Z. We thank Nick Cull (UEA) for technical assistance.

■ REFERENCES

(1) Lancaster, J. R., Jr. *Nitric Oxide* **1997,** *1*, 18–30.
(2) Cooper, C. E. *Biochim. Biophys. Acta* **1999,** *1411*, 290–309.
(3) Bruckdorfer, R. *Mol. Aspects Med.* **2005,** *26*, 3–31.
(4) Watmough, N. J.; Butland, G.; Cheesman, M. R.; Moir, J. W.; Richardson, D. J.; Spiro, S. *Biochim. Biophys. Acta* **1999,** *1411*, 456–474.
(5) Poole, R. K. *Biochem. Soc. Trans.* **2005,** *33*, 176–180.
(6) Broillet, M. C. *Cell. Mol. Life Sci.* **1999,** *55*, 1036–1042.
(7) Rhee, K. Y.; Erdjument-Bromage, H.; Tempst, P.; Nathan, C. F. *Proc. Natl. Acad. Sci. U.S.A.* **2005,** *102*, 467–72.
(8) Kwon, Y. M.; Weiss, B. *J. Bacteriol.* **2009,** *191*, 5369–5376.
(9) Weiss, B. *J. Bacteriol.* **2006,** *188*, 829–833.
(10) Nakane, M. *Clin. Chem. Lab. Med.* **2003,** *41*, 865–870.
(11) Pullan, S. T.; Gidley, M. D.; Jones, R. A.; Barrett, J.; Stevanin, T. M.; Read, R. C.; Green, J.; Poole, R. K. *J. Bacteriol.* **2007,** *189*, 1845–1855.
(12) Bodenmiller, D. M.; Spiro, S. *J. Bacteriol.* **2006,** *188*, 874–881.
(13) Tucker, N. P.; Hicks, M. G.; Clarke, T. A.; Crack, J. C.; Chandra, G.; Le Brun, N. E.; Dixon, R.; Hutchings, M. I. *PLoS One* **2008,** *3*, e3623.
(14) Ding, H.; Demple, B. *Proc. Natl. Acad. Sci. U.S.A.* **2000,** *97*, 5146–5150.
(15) Cruz-Ramos, H.; Crack, J.; Wu, G.; Hughes, M. N.; Scott, C.; Thomson, A. J.; Green, J.; Poole, R. K. *EMBO J.* **2002,** *21*, 3235–3244.
(16) Drapier, J. C. *Methods* **1997,** *11*, 319–329.
(17) Costanzo, S.; Menage, S.; Purrello, R.; Bonomo, R. P.; Fontecave, M. *Inorg. Chim. Acta* **2001,** *318*, 1–7.
(18) Pieper, G. M.; Halligan, N. L.; Hilton, G.; Konorev, E. A.; Felix, C. C.; Roza, A. M.; Adams, M. B.; Griffith, O. W. *Proc. Natl. Acad. Sci. U. S.A.* **2003,** *100*, 3125–3130.
(19) Kennedy, M. C.; Antholine, W. E.; Beinert, H. *J. Biol. Chem.* **1997,** *272*, 20340–20347.
(20) Sellers, V. M.; Johnson, M. K.; Dailey, H. A. *Biochemistry* **1996,** *35*, 2699–2704.
(21) Duan, X.; Yang, J.; Ren, B.; Tan, G.; Ding, H. *Biochem. J.* **2009,** *417*, 783–789.
(22) Foster, H. W.; Cowan, J. A. *J. Am. Chem. Soc.* **1999,** *121*, 4093–4100.
(23) Butler, A. R.; Glidewell, C.; Li, M. *Adv. Inorg. Chem.* **1988,** *32*, 335–393.
(24) Tucker, N. P.; Le Brun, N. E.; Dixon, R.; Hutchings, M. I. *Trends Microbiol.* **2010,** *18*, 149–156.
(25) Molle, V.; Palframan, W. J.; Findlay, K. C.; Buttner, M. J. *J. Bacteriol.* **2000,** *182*, 1286–1295.
(26) Jakimowicz, P.; Cheesman, M. R.; Bishai, W. R.; Chater, K. F.; Thomson, A. J.; Buttner, M. J. *J. Biol. Chem.* **2005,** *280*, 8309–8315.
(27) Crack, J. C.; den Hengst, C. D.; Jakimowicz, P.; Subramanian, S.; Johnson, M. K.; Buttner, M. J.; Thomson, A. J.; Le Brun, N. E. *Biochemistry* **2009,** *48*, 12252–12264.
(28) Kang, S. H.; Huang, J.; Lee, H. N.; Hur, Y. A.; Cohen, S. N.; Kim, E. S. *J. Bacteriol.* **2007,** *189*, 4315–4319.
(29) Morris, R. P.; Nguyen, L.; Gatfield, J.; Visconti, K.; Nguyen, K.; Schnappinger, D.; Ehrt, S.; Liu, Y.; Heifets, L.; Pieters, J.; Schoolnik, G.; Thompson, C. J. *Proc. Natl. Acad. Sci. U.S.A.* **2005,** *102*, 12200–12205.
(30) Banaiee, N.; Jacobs, W. R., Jr.; Ernst, J. D. *Infect. Immun.* **2006,** *74*, 6449–6457.
(31) Rohde, K. H.; Abramovitch, R. B.; Russell, D. G. *Cell Host Microbe* **2007,** *2*, 352–364.
(32) Daniel, J.; Deb, C.; Dubey, V. S.; Sirakova, T. D.; Abomoelak, B.; Morbidoni, H. R.; Kolattukudy, P. E. *J. Bacteriol.* **2004,** *186*, 5017–5030.
(33) Sirakova, T. D.; Dubey, V. S.; Deb, C.; Daniel, J.; Korotkova, T. A.; Abomoelak, B.; Kolattukudy, P. E. *Microbiology* **2006,** *152*, 2717–2725.
(34) Singh, A.; Crossman, D. K.; Mai, D.; Guidry, L.; Voskuil, M. I.; Renfrow, M. B.; Steyn, A. J. *PLoS Pathog.* **2009,** *5*, e1000545.
(35) Singh, A.; Guidry, L.; Narasimhulu, K. V.; Mai, D.; Trombley, J.; Redding, K. E.; Giles, G. I.; Lancaster, J. R., Jr.; Steyn, A. J. *Proc. Natl. Acad. Sci. U.S.A.* **2007,** *104*, 11562–11567.
(36) Smith, L.; Stapleton, M. R.; Fullstone, G.; Crack, J.; Thomson, A. J.; Le Brun, N. E.; Hunt, D.; Harvey, E.; Adinolfi, S.; Buxton, R. S.; Green, J. *Biochem. J.* **2010,** *432*, 417–427.
(37) Alam, M. S.; Garg, S. K.; Agrawal, P. *Mol. Microbiol.* **2007,** *63*, 1414–1431.
(38) Sorbo, B.; Heyman, T. *Biochim. Biophys. Acta* **1957,** *23*, 624–627.
(39) Petering, D.; Fee, J. A.; Palmer, G. *J. Biol. Chem.* **1971,** *246*, 643–653.
(40) Bradford, M. M. *Anal. Biochem.* **1976,** *72*, 248–254.
(41) Crack, J. C.; Green, J.; Le Brun, N. E.; Thomson, A. J. *J. Biol. Chem.* **2006,** *281*, 18909–18913.
(42) Beinert, H. *Anal. Biochem.* **1983,** *131*, 373–8.
(43) Gergel, D.; Cederbaum, A. I. *Arch. Biochem. Biophys.* **1997,** *347*, 282–288.
(44) Kuzmic, P. *Methods Enzymol.* **2009,** *467*, 247–280.
(45) Becke, A. D. *J. Chem. Phys.* **1993,** *98*, 5648–5652.
(46) Lee, C.; Yang, W.; Parr, R. G. *Phys. Rev. B* **1988,** *37*, 785–789.
(47) Hay, P. J.; Wadt, W. R. *J. Chem. Phys.* **1985,** *82*, 270–283.
(48) Wadt, W. R.; Hay, P. J. *J. Chem. Phys.* **1985,** *82*, 284–298.
(49) Couty, M.; Hall, M. B. *J. Comput. Chem.* **1996,** *17*, 1359–1370.
(50) Check, C. E.; Faust, T. O.; Bailey, J. M.; Wright, B. J.; Gilbert, T. M.; Sunderlin, L. S. *J. Phys. Chem. A* **2001,** *105*, 8111–8116.
(51) Tonzetich, Z. J.; Wang, H.; Mitra, D.; Tinberg, C. E.; Do, L. H.; Jenney, F. E., Jr.; Adams, M. W.; Cramer, S. P.; Lippard, S. J. *J. Am. Chem. Soc.* **2010,** *132*, 6914–6916.
(52) Harrop, T. C.; Tonzetich, Z. J.; Reisner, E.; Lippard, S. J. *J. Am. Chem. Soc.* **2008,** *130*, 15602–15610.
(53) Wang, R.; Camacho-Fernandez, M. A.; Xu, W.; Zhang, J.; Li, L. *Dalton Trans.* **2009,** 777–786.
(54) Glidewell, C.; Hyde, A. R. *Polyhedron* **1985,** *4*, 1155–1158.
(55) Butler, A. R.; Glidewell, C.; Johnson, I. L. *Polyhedron* **1987,** *6*, 1147–1148.
(56) Glidewell, C.; Johnson, I. L. *Chem. Scr.* **1987,** *27*, 441–444.
(57) den Hengst, C. D.; Buttner, M. J. *Biochim. Biophys. Acta* **2008,** *1780*, 1201–1216.
(58) Alam, M. S.; Garg, S. K.; Agrawal, P. *FEBS J.* **2009,** *276*, 76–93.
(59) Nashef, A. S.; Osuga, D. T.; Feeney, R. E. *Anal. Biochem.* **1977,** *79*, 394–405.